Title	Investigation of histology region in dielectric measurements of heterogeneous tissues
Author(s)	Porter, Emily; O'Halloran, Martin
Publication Date	2017-08-17
Publication Information	Porter, E., & O'Halloran, M. (2017). Investigation of Histology Region in Dielectric Measurements of Heterogeneous Tissues. IEEE Transactions on Antennas and Propagation, 65(10), 5541-5552. doi: 10.1109/TAP.2017.2741026
Publisher	Institute of Electrical and Electronics Engineers (IEEE)
Link to publisher's version	http://dx.doi.org/10.1109/TAP.2017.2741026
Item record	http://hdl.handle.net/10379/7217
DOI	http://dx.doi.org/10.1109/TAP.2017.2741026

Investigation of Histology Region in Dielectric Measurements of Heterogeneous Tissues

Emily Porter*, *Member, IEEE*, and Martin O'Halloran, *Member, IEEE*

***Abstract*—The dielectric properties of tissues are key parameters in electromagnetic medical technologies. Despite the apparent simplicity of the dielectric measurement process, reported data has been inconsistent for heterogeneous tissues. Dielectric properties may be attributed to heterogeneous tissues by identifying the tissue types that contributed to the measurement through histological analysis. However, accurate interpretation of the measurements with histological analysis requires first defining an appropriate histology region to examine. Here, we investigate multiple definitions for the probe sensing depth and uniquely calculate this parameter for measurements with a realistic range of tissues. We demonstrate that different sensing depth definitions are not equivalent, and may introduce error in dielectric data. Lastly, we propose an improved definition, given by the depth to which the probe can detect changes in the tissue sample, within the measurement uncertainty. We equate this sensing depth with histology depth, thus supporting the need of having the tissue region that contributes to the dielectric data be the same as that which is analysed histologically. This study demonstrates that, for these tissues, the histology depth is both frequency and tissue dependent. Therefore, the histology depth should be selected based on the measurement scenario, otherwise inaccuracies in the data may result.**

***Index Terms*—Biological materials, dielectric measurement, open-ended coaxial probe, tissue properties.**

I. Introduction

Dielectric properties are an inherent characteristic of biological tissues. These properties dictate how electromagnetic (EM) waves are reflected, absorbed, and transmitted in all materials, including tissues. The dielectric properties of tissues are known to be both frequency- and temperature-dependent [1]-[4]. These tissue properties are used in dosimetry studies to determine safe levels of exposure to EM fields with wireless devices, wearable, and on-body technologies. The properties are also highly relevant to existing medical techniques and vital to the design and development of novel EM medical devices for diagnostics, monitoring, and therapeutics.

Specifically, an understanding of the local tissue heterogeneity is of importance in balancing safety requirements with treatment efficacy in EM therapeutic techniques such as ablation and hyperthermia [5]-[11]. Similarly, in diagnostic imaging, the properties of tissues must be known well enough to determine whether there is a contrast between the background tissue and the tissue of interest. The dielectric contrast has especially been of concern in the field of microwave breast imaging [12], where new information on the contrast between the malignant and healthy tissues [13], [14], has dampened the likelihood of developing a successful imaging tool using this technology.

Heterogeneous tissues are samples or organs that contain multiple (2+) types of tissues within them. In this study, any bulk sample that contains more than one type of tissue is considered to be heterogeneous. Homogeneous tissues, on the other hand, are tissue samples or organs that are composed of only one tissue type. Historically, the dielectric properties of heterogeneous tissues have been quantified through repeated measurements of different samples. This type of analysis provides the mean and variation in the dielectric properties for the bulk heterogeneous tissue in question [15]. However, a localized understanding of the heterogeneous tissue composition is becoming increasingly important. As a result, modern dielectric studies often perform histological analysis in order to determine the tissue types that are present within the sample and/or to verify if the sample contains diseased tissue [13], [14], [16], [17]. However, in order to conduct a histological analysis of a tissue sample, the region of the tissue sample subject to analysis should be defined. This 'histology region' delimits the volume of tissue that is to be investigated in relation to the dielectric property measurement. This region is a key factor in attributing dielectric property measurements correctly to the tissues that have contributed to them, especially with heterogeneous tissues. Despite the importance of this region, there is no consistent definition of the histology radius or depth in the literature, and no agreement on how these important parameters could be determined. As a result, it is difficult to reliably compare dielectric data across studies. This factor may partially explain why dielectric measurements of the same types of tissues from the literature are not always in agreement [14], [18], [19]. This discrepancy in reported dielectric properties causes difficulties for those developing medical devices, as it is not clear which data set is the most appropriate to use. However, once a histology region is identified, mixture models can be used to relate the effective (measured) permittivity to the permittivity of the constituent

Date submitted: Nov. 15, 2016. The research leading to these results has received funding from the European Research Council under the European Union's Horizon 2020 Programme/ ERC Grant Agreement BioElecPro n. 637780, the Natural Sciences and Engineering Research Council of Canada (NSERC), and the Irish Research Council (IRC) New Foundations Award. This work has been developed in the framework of COST Action MiMed (TD1301).

The authors are with the National University of Ireland Galway, Ireland (correspondence email: emily.porter@nuigalway.ie).

tissues of the sample and vice versa [16], [20]. Alternately, and as is the focus in this work, the histology region can be used to interpret the dielectric data in the context of the tissue types that have resulted in that dielectric measurement. In dielectric measurement studies on tissues, open-ended coaxial probes have become the de facto measurement technique [21]. Therefore, this work focuses only on measurements with open-ended coaxial probes.

In the past, the sensing depth of the probe has usually been estimated on homogeneous materials and considered as a fixed volume regardless of the tissue composition within a given sample [13], [14], [22], [23]. Yet recent studies may suggest that the depth that meaningfully contributes to dielectric measurements is significantly less than previously thought, and that the tissue directly in front of the probe tip has a dominant effect on the measured data [24]. However, what defines a 'meaningful contribution' is still an open question.

In this work, we aim to develop a foundation for finding the appropriate histology depth to demarcate slices of tissue for histological analysis in order to obtain accurate dielectric property measurements. We investigate and compare candidate histology depth definitions from the literature (including both sensing depth and penetration depth definitions) and combine key features of existing definitions to obtain one that can be applied widely across applications and measurement scenarios. Notably, we perform measurements on sets of tissue-mimicking phantoms and on actual biological tissue samples. As a result, we are able to examine the histology depth in situations that are as realistic as possible: with the range of material dielectric properties and contrasts that are representative of those found in human biological tissues. To our knowledge, a histology depth study has never before been conducted under such realistic conditions. We further examine whether the magnitude of the dielectric properties, the dielectric contrast, and the measurement frequency impact the depth calculation for each definition. For each of these potential factors of variation, we quantify the magnitude of the effect introduced in the histology depth and determine whether it is significant or not.

We note that in this study, we focus only on the histology depth. The histology radius is also relevant in determining the full histology volume – this parameter is to be investigated in future work. In the next section, we provide background information that is required to fully contextualize this study. We highlight the importance of the histology depth in dielectric measurement of tissues, and describe existing studies that have examined the depth parameter. In Section III, we describe the experimental measurement system, measurement validation, and the various measurement scenarios. In Section IV, the materials used in the dielectric measurements are described. Then, in Section V, we introduce the candidate histology depth definitions. Finally, Section VI provides the measurement results and corresponding analysis, while Section VII concludes the paper.

II. Background

A. The Importance of Histology Depth

The histology depth is the distance into a tissue sample that should be included in histological analysis. Appropriate determination of this depth is vital to correctly interpreting the measured dielectric properties. The histology depth is of utmost importance when heterogeneous tissues are being measured. When homogeneous tissues are under investigation, it is only necessary to ensure that the sample is large enough that reflections from the edges of the sample are negligible. However, with heterogeneous tissues, histology is typically performed after dielectric measurements to determine the sample composition (i.e., which specific tissue types are present and their relative distribution). In this case, the histology depth must be precisely known in order to accurately interpret the results.

As an example of the significance and importance of the histology depth in dielectric measurements, Fig. 1 illustrates a histology slice from an actual tissue sample. In this tissue slice, several constituent tissues are visible as evidenced by the different colour levels in the applied hematoxylin and eosin (H&E) stain (white to purple to dark red). With different histology region areas (denoted r_1 and r_2), the amounts and types of tissues within the region vary considerably. As a result, a dielectric measurement that is interpreted through histological analysis can only be interpreted meaningfully if the appropriate histology region is used. Otherwise, the dielectric measurement does not correspond to the tissue types that have resulted in those dielectric properties.

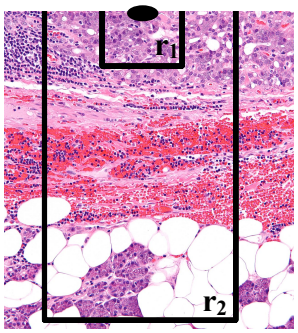

Fig. 1. Photograph of a histology slice containing a heterogeneous sample of tissues (adapted from [25]). This sample is considered heterogeneous as it contains multiple types of tissues within it. The dielectric probe measurement location is marked with the black circle. Two histology regions are marked, a smaller region r_1 and a larger one r_2. This indicates how significantly different the tissues counted as contributing to the dielectric property measurement may be, depending on the histology region used.

A further, more straightforward, example focuses on the histology depth factor alone. A diagram of a simplified tissue sample is provided in Fig. 2. The tissue sample is heterogeneous, composed partially of Tissue 1 and partially of Tissue 2. In this situation, if the histology depth is labeled as d_1, then the region is entirely filled by Tissue 2 – thus, only Tissue 2 is considered as contributing to the dielectric property measurement. On the other hand, if the histology depth is calculated to be d_3, then the region contains Tissue 2 and a portion of Tissue 1 – both of which contribute to the analysis. As is illustrated in this example, knowledge of how to identify

the histology depth is necessary in order to determine which parts of the tissue sample should be analysed. As a result, the interpretation of the dielectric property measurement (which is dependent on the tissue composition that has resulted in the given measurement data) also depends on the histology depth. We note that this example is highly simplified, and in reality a sample may contain multiple tissue types existing simultaneously at each depth.

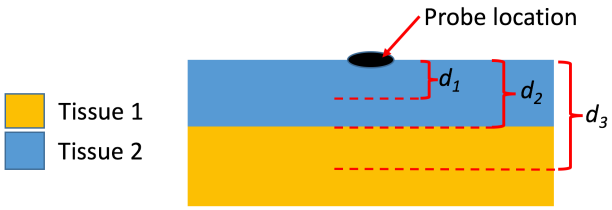

Fig. 2. Diagram of a simplified tissue sample containing two tissue layers. This bulk tissue sample is heterogeneous (contains more than one tissue type); whereas each individual layer is homogeneous (contains only one tissue type). Tissue 1 (yellow) is at the bottom of the sample and Tissue 2 (blue) is at the top of the sample, in contact with the probe (the slim form probe diameter is 2.2 mm [23]). The thickness of Tissue 2 is given by d_2. The interpretation of the measured dielectric properties in this situation will change based on which value (for example, d_1 *or* d_3) is taken as the histology depth.

B. Depth Calculations in Existing Studies

While the histology depth concept seems straightforward, there are several factors that complicate matters. For instance, it is possible that the frequency of the measurement and the dielectric properties of the materials being measured, could have an effect on the histology depth. The sample composition is of particular concern with heterogeneous samples. Further, there is yet to be a consensus in the literature on the definition of this depth, or even for the name of this parameter. In this section, we review key studies in the literature that have examined parameters relevant to the histology depth of open-ended coaxial probes in inhomogeneous measurement scenarios. We further discuss the definition of each depth-related parameter, and how the experiment was performed for each study.

In [22], the 'sensing depth' was investigated in order to determine the size of a sample for which reflections from the edge of the sample do not affect measurement results. This study used a custom-made 2.2 mm diameter probe immersed in a standard liquid held in a glass beaker. The study was performed over 1 – 20 GHz, with standard reference liquids representing the range of dielectric properties of the various breast tissues. The extent of the sensing depth was given by the larger of two distances from the probe tip to the beaker bottom: i) the distance at which the real part of the permittivity differed from real permittivity of the reference location by ±10%; or ii) the distance at which the imaginary part differed by ±10%. The sensing depth, according to this definition, was found to be approximately 0.75 – 1 mm for ethanol, 1 – 1.5 mm for methanol, and 1.5 mm for deionised water. This result suggests that the sensing depth increases as the contrast in dielectric properties increases. Similarly, with a larger diameter probe (3.58 mm), the sensing depth was found to be between 1.25 – 3 mm for these materials. The sensing depth was not found to vary significantly with frequency. The results of this work were used in the well-known large-scale dielectric property studies of healthy and malignant breast tissues in [13], [14]. In these studies, a different custom probe was used with similar diameter (3 mm) to the probe in [22]; thus, the larger estimated sensing depth of 3 mm was used in the histological analysis of the heterogeneous breast tissues.

In another series of studies, [19] and [24], the 'penetration depth' was investigated in the context of two-layer material compositions. The motivation for these works was the idea that the dielectric properties are disproportionately and dominantly affected by the material directly at the probe tip, as opposed to proportionally affected by the materials throughout the sensing volume. In [24], this result was investigated comprehensively. A new term, the 'effective penetration depth', was defined to describe the region where both of the two-layer materials have representative influence on the measured dielectric properties [24]. With measurements on Teflon and water, the effective penetration depth was found to be only 0.28 mm, significantly less than 3 mm. This indicates that extreme care should be taken when interpreting the dielectric measurement of heterogeneous tissues, as the material properties closest to the probe must be weighted relative to those further away. Further, it was found that the penetration depth is relatively constant with respect to frequency (0.5 – 10 GHz) and material properties, but varies with probe diameter [24].

Each of these existing studies has given great insight into the sample region that may be considered for histological analysis. However, the investigated scenarios have been simplified relative to the complexity of dealing with heterogeneous tissues. Further, many of the existing studies utilize parameters that are arbitrarily selected. Therefore, questions remain regarding how the histology depth should be defined for a given investigation, and whether or not it is dependent on material properties and frequency. These questions are of significant concern when dealing with complex heterogeneous tissues.

III. Measurements

In this section, the dielectric measurement system is introduced and described. Then, the technique for validating the system performance is detailed and the calculated uncertainty presented. Measurements performed to enable comparison and verification with the literature are discussed. Finally, measurements performed on tissue-mimicking phantom materials with realistic dielectric properties and dielectric contrast are overviewed, along with measurements conducted using biological tissue samples. For phantom and tissue experiments, care was taken to select materials with dielectric properties and contrasts that span the expected values of human tissues.

A. Dielectric Measurement System

In this measurement study we used the Keysight slim form probe (diameter 2.2 mm) [23] connected to the Agilent E5063A network analyser. This small diameter probe was selected for this study because it has been the most commonly

used in recent studies of tissue properties [16], [17], [26], [27]. For all measurements, 101 frequency points were taken over the range of 300 MHz – 8.5 GHz. This band was chosen as it covers the frequency range of interest for microwave breast imaging and diagnostic systems. As the breast is the most heterogeneous organ typically investigated, the question of sensing depth in this scenario is highly relevant.

We note that the Keysight slim form probe is designed for operation at frequencies above 500 MHz. However, this probe has been used in the literature at frequencies below 500 MHz, and as low as 100 MHz [19], [24]. In this study, we performed validation measurements (discussed in more detail in Section III.B), and confirmed that the measurement accuracy is high at frequencies down to 300 MHz, and therefore we are able to include the lower frequencies in this study.

The probe was calibrated using a three-load standard calibration. In this case, open-circuit, short-circuit, and a broadband load of deionised water were used for all calibrations. The network analyser was turned on and warmed up for at least 24 hours prior to each calibration and measurement. Measurements with all materials were performed at room temperature (22˚C) in a controlled room.

In order to perform dielectric measurements to characterise the histology depth in a repeatable way, a measurement chamber was designed. This chamber is roughly based on the tank in [24], although we have modified the design to suit this series of experiments. A diagram depicting the chamber and its components is shown in Fig. 3, and a photograph of the setup in Fig. 4. The concept is to be able to measure the effect of a material at different distances from the probe tip, thereby gauging how distance from a material impacts the measured data.

The chamber was built as a cylindrical tube of acrylic, with a height of 30 cm and a diameter of 20 cm. As can be seen in Figs. 3 and 4, the probe is fixed at the bottom of the chamber. The hole through which the probe was inserted into the chamber was sealed to prevent leakage. In this way, the probe was fixed in place while the other components move – thus minimising both cable movement and repeatability errors. The probe was immersed in a liquid, denoted as 'Material 2'. At the top of the chamber, a micrometer is attached to a solid, 'Material 1'. The micrometer enables both the movement of Material 1 in the vertical direction, and recording of the position of this material (i.e., the depth). For all measurement scenarios, the thickness of Material 1 is greater than 1 cm (large enough so that the edges of the tissue do not impact the dielectric measurement).

During a measurement set, Material 1 is lowered such that it is in good contact with the probe. The depth, d, at contact is the origin of the measurement (d = 0 mm). At this position, Material 1 occupies the full histology region of the probe. Then, Material 1 is moved away from the probes in discrete increments, up to several mm. Specifically, as Material 1 is moved away, the thickness of Material 2 varies from 0 mm to 15 mm. At the largest thickness of Material 2, Material 2 occupies the entire histology region of the probe. At each position, a measurement of the dielectric properties is recorded. We note that Material 1, as the solid, has a fixed thickness over each measurement set. For Material 2, as the liquid, the thickness changes for each measurement within the set.

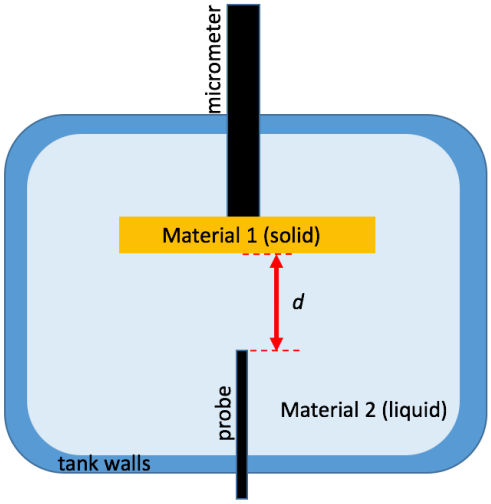

Fig. 3. Diagram of the measurement chamber. A micrometer is attached to Material 1, which is moved toward and away from the probe. The chamber is filled with liquid Material 2. As Material 1 is moved, the distance d between the probe and Material 1 (i.e., the thickness of Material 2) changes.

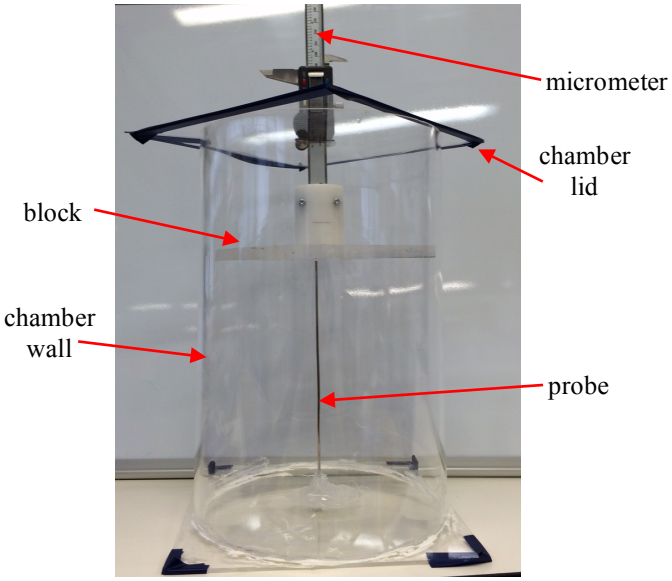

Fig. 4. Photograph of the measurement chamber. The micrometer is fixed to the lid of the chamber with the end of it attached to Material 1 (the block shown in this image), enabling vertical movement and recording of the depth. The probe enters through the bottom of the chamber.

B. *Measurement Validation*

We validate the measurement system by performing measurements on a material with well-known dielectric properties, 0.1 M NaCl (saline). This validation material was chosen for the following reasons: *i)* the dielectric properties are well-characterised with accurate models available over our frequency range of interest; *ii)* the conductivity and permittivity are of the same order as those of biological tissues [28]; and *iii)* saline is easily obtainable and does not require special handling procedures.

In order to characterise the uncertainty in the system, we take repeated measurements on the validation material. In particular, we performed 15 measurements over three calibrations of the network analyser. The measurements were taken at 22ºC.

First, we compared the measured data to the known model of saline at both 300 MHz and 500 MHz, in order to confirm that operation of the probe at 300 MHz is justified. At each frequency point, we calculated the percent error between the model and the measured data. It was found that the difference in percent error between data from 500 MHz and data from 300 MHz was less than 0.25%. Therefore, measurements at 300 MHz are very similar in accuracy level to measurements at 500 MHz, and we can be confident that use of the probe at lower frequencies down to 300 MHz is appropriate.

Next, these validation measurements were used to calculate the total combined uncertainty (across all frequencies), as in [28], based on the National Institute of Standards and Technology (NIST) guidelines [29]. With this method, the total combined uncertainty (TCU) is calculated as the square root of the sum of squared individual uncertainties. In this study, the individual uncertainties include the repeatability (Type A error), which indicates the random errors present in a measurement; the accuracy (Type B error), which gives the offset in the mean measured values relative to the known material properties (i.e., systematic errors); and the error due to cable movement. Drift was not included in this calculation as each measurement presented in this work was performed immediately following a calibration and thus the error due to drift was negligible.

The errors are calculated for each measured parameter separately. The TCU for the relative permittivity, ε_r, is found to be 2.1, while the TCU for conductivity, σ, is 3.4. In particular, for ε_r, the repeatability is within 2.1% and the accuracy is within 0.26%. For σ, the repeatability in the measurement is within 2.3% and the accuracy is within 4.2%. In this case, we recommend using ε_r to determine the histology depth as the uncertainty of the measurement is lower than for conductivity.

C. Standard Experiments from the Literature

Two experiments are performed prior to conducting tests with biological tissues and tissue-mimicking materials. These experiments are performed in order to enable comparison with other results presented in the literature.

The first experiment, presented in [22] and discussed in detail in Section II, involves the probe immersed in a liquid (in this case, deionised water) in a glass beaker. We repeat this measurement with our system, and calculate the sensing depth using the definition in [22]. We use the same beaker type (600 mL volume) and liquid (deionised water) as in [22]. Our measurements found general agreement with the result of 1.5 mm in [22], with the sensing depth calculated to be between 1.05 – 1.41 mm. We note that direct comparison cannot be made to the results in [22], as we use a commercial probe whereas in [22] a custom probe was used. However, while the probes may have been built with different materials, they both have the same diameter (2.2 mm), so similar sensing depths would be expected. Further, the exact water temperature during the measurement is not stated in [22], and there may be slight impact on the comparison if our measurement and the measurement in [22] were performed at different temperatures.

The second experiment that we conduct is a replication of the one presented in [24] and summarised in Section II. With a two-layered experiment of Teflon and deionised water, the penetration depth for the coaxial probe was found to be 0.28 mm at 300 MHz. We repeated this experiment using the same type of dielectric probe as in [24] and the same type of materials. While an exact comparison is not possible due to sources of variation introduced between studies, including differences in water temperature and the material properties of the specific Teflon samples used, we also found the depth to be significantly less than 1 mm. We note that the trend, i.e., the shape of the curve of relative permittivity vs. distance for a fixed frequency, was also consistent with that in [24].

We also performed a final validation experiment in order to determine the minimum thickness of Material 1. In [24], the thickness of the Teflon was 1 cm. To verify that this material thickness was sufficient such that reflections from the edges of the material were not contaminating the measured data, we performed a series of measurements on acrylic and Teflon, each in 1 cm thick and 7 cm thick blocks. Ten measurements on each block were taken over 300 MHz – 8.5 GHz. All four blocks were backed by a (highly reflective) metal foil during the measurements. We found no statistically significant difference in the dielectric properties of the 7 cm thick block relative to the 1 cm thick block for either material. Thus, a 1 cm sample thickness is determined to be sufficient and will be used in this study as well.

D. Measurement Summary

The measurements that we conducted with tissues and phantoms are summarised in Table I. These measurements cover the range of expected permittivity values and permittivity contrasts that may be found in biological tissue samples. These measurements also contain scenarios in which the probe is in contact with a high permittivity material with a low permittivity material behind it, and vice versa.

The composition of the experimental data is as follows.

- Each experimental scenario is defined as a ‘Set’. A Set is defined by the Materials 1 and 2 that are used. For each Set, multiple measurements are taken.
- Within a Set, measurements are performed to collect the complex permittivity versus frequency for each depth *d*. One full data array is a collection of measurements across all depth points.
- For each Set, at least 15 full data arrays are collected.

Data arrays that do not contain depth points at the locations needed to define the curves in the permittivity versus distance plots (as in Fig. 5), are excluded from further analysis as they do not contain enough information to accurately calculate the histology depth. The remaining arrays are incorporated to obtain one per Set. For example, in Set #6, data for 18 arrays was collected (each of permittivity across frequency and depth). In the first array, 25 measurements were taken at various depths *d*, in the second array 23 measurements were taken, and so on; thus, more than 250 individual measurements make up Set #6. As the depth control is manual, the exact value and number of the depth points is not the same

within each Set or across Sets. The depth points are concentrated in regions where the change in permittivity is highest.

TABLE I. SUMMARY OF MEASUREMENTS PERFORMED WITH TISSUE-MIMICKING PHANTOMS AND ACTUAL TISSUE SAMPLES. THE REFINED FAT IS DENOTED SOLELY AS "FAT".

Set #	Type	Material 1	Material 2	Contrast
#1	Phantom	Rubber A	0.9% Saline	High
#2	Phantom	Rubber B	0.9% Saline	Low
#3	Phantom+Tissue	Rubber A	Fat	Low
#4	Phantom+Tissue	Rubber B	Fat	High
#5	Tissue	Porcine Muscle	Fat	High
#6	Tissue	Porcine Fat	Fat	Low

IV. MATERIALS

In this section, the materials that are used in each measurement scenario are presented. For each scenario, the motivation is provided, along with all relevant parameters (materials, properties, dimensions, etc.).

A. Phantom Materials

Phantom materials are investigated as they offer dielectric properties and contrasts that match those of biological tissues, without any of the additional challenges associated with tissue sources, handling, and uncertain material properties. The solid tissue-mimicking phantoms used in this study are made of carbon black and rubber, in varying proportions. The details of these phantoms, based on the phantoms in [30], can be found in [31]. The phantoms are stable and durable – making them perfect for the study presented in this work.

We denote the two phantom types as 'Rubber A' and 'Rubber B'. Rubber A is a low-permittivity, fat-mimicking phantom ($\varepsilon_r \approx 7$ at 5 GHz). Rubber B is of higher permittivity, and mimics breast glandular tissue, according to the measured properties in [14] ($\varepsilon_r \approx 52$ at 5 GHz). All samples have dimensions larger than 2 cm^3.

A liquid phantom of physiological (0.9% or 0.124M) saline is also used in the experiments. Its properties are close to the upper limit of biological tissue properties; for example, they match closely with malignant breast tissue properties [14] ($\varepsilon_r \approx 72$ at 5 GHz and 24ºC).

B. Biological Tissue Materials

Biological tissues are investigated in order to confirm the depth trends that are established with phantom materials. Three types of tissue samples are obtained for this study. We use porcine fat and muscle samples as the solid samples (Material 1 in Fig. 2), and refined fat as the liquid sample (Material 2 in Fig. 2). The porcine samples were obtained from an abattoir, and were sliced to the thickness required for this study, with no additional preparation or processing. We note that while each porcine sample is approximately homogeneous, no actual tissue samples are perfectly homogeneous due to inherent biological variability. The refined fat sample originates from animal fat as well, but was processed to remove impurities, resulting in a sample that has a higher level of homogeneity than natural fatty tissue. The porcine muscle sample has high permittivity, while the fat tissues both have lower permittivity, with the refined fat having lower permittivity than the porcine fat (presumably, due to it being purer fat). In particular, at 5 GHz, the porcine fat has $\varepsilon_r \approx 11$, the refined fat has $\varepsilon_r \approx 2.5$. The muscle sample has $\varepsilon_r \approx 46$.

We note that all ethical guidelines were followed in procurement of these tissue samples and in conducting this study.

V. CANDIDATE HISTOLOGY DEPTH DEFINITIONS

In this section, potential candidate definitions for defining the histology depth are also presented. Specifically, five candidate histology depth definitions are considered in this work. These candidates include both 'sensing depth' and 'penetration depth' definitions, either of which may reasonably be used as the histology depth. There are subtle differences between some of the definitions; however, the differences do have an impact on the calculated depth value. Definitions 1) and 3) are from the literature, whereas definitions 2), 4), and 5) are logical variants that are uniquely discussed in this work.

The definitions are detailed below.

1) Sensing depth from [22]

The sensing depth, $d_{s\_10\%}$, is defined as the depth at which the measured dielectric properties deviate from the properties of Material 2 by more than 10%, for any given frequency. This definition was explained in detail in Section II.B.

2) Modified version of sensing depth from 1)

The sensing depth at which, within the uncertainty (μ) of the system, the contribution of Material 1 to the measured dielectric properties ceases to be discernable. In other words, at this depth, the presence of Material 1 is no longer detectable. Denoted as d_{s_μ}, this is the depth that indicates the minimum size of a homogeneous sample to avoid reflections from the edges of the sample.

3) Penetration depth from [24]

The penetration depth, as defined in [24] and discussed in Section II.B., is the depth over which both materials are represented somewhat proportionally. This depth, $d_{p\_20\%}$, is given by the distance at which the curve of measured properties versus distance deviates from a straight line by 20%. In this work, the fitted straight line is the line that has the best R^2-coefficient with the curve, and that contains the inflection point of the curve. We note that we have adapted this definition for use with tissue materials: since the tissue is soft, the probe was pushed slightly into the tissue in order to maintain good contact. Thus, we see a deviation from the straight line at depths when the probe is close to being in contact with Material 1, and when it is surrounded mostly by Material 2. We apply the 20% deviation criteria to both the upper and lower portions of the curve. In this case, the depth value demarcates a region in between both tissues, but that touches neither.

4) Modified version of penetration depth from 3)

The modified penetration depth, d_{p_μ}, is given by the depth at which the curve of measured properties versus distance deviates from a straight line by greater than the measurement uncertainty.

5) Sensing region reframed

In order to interpret measurements on heterogeneous samples, the depth considered should include contributions from both tissue types, as in definition 3). However, it is not necessary for the contributions to be proportional in order to have a reliable analysis. Thus, we define the region of depths in which both Material 1 and Material 2 are detectable, i.e., their contribution to the measured dielectric properties is outside the uncertainty. This depth is labeled d_{comb_μ}.

The definitions that have been described above are illustrated graphically in Fig. 5. Specifically, Fig. 5(a) highlights the definitions 1), 2), and 5); and Fig. 5(b) illustrates definitions 3) and 4). In Fig. 5, an example of measured relative permittivity is plotted versus distance for a fixed frequency. The bottom horizontal part of this curve indicates the properties of Material 1, which is initially in contact with the probe. The upper horizontal part of the curve is the permittivity of Material 2. At distances in between the two horizontal sections, the dielectric properties of both materials are contributing to the measured data.

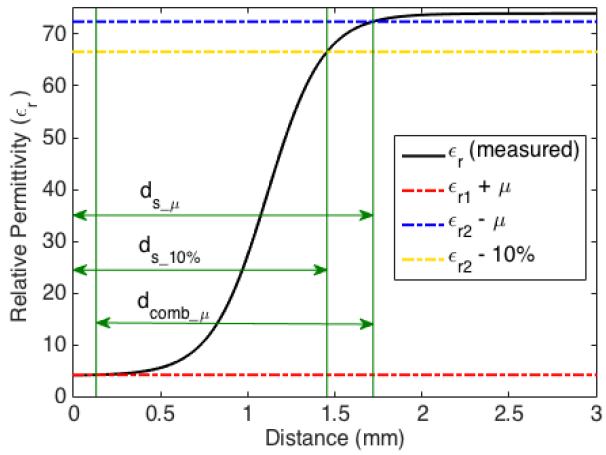

(a)

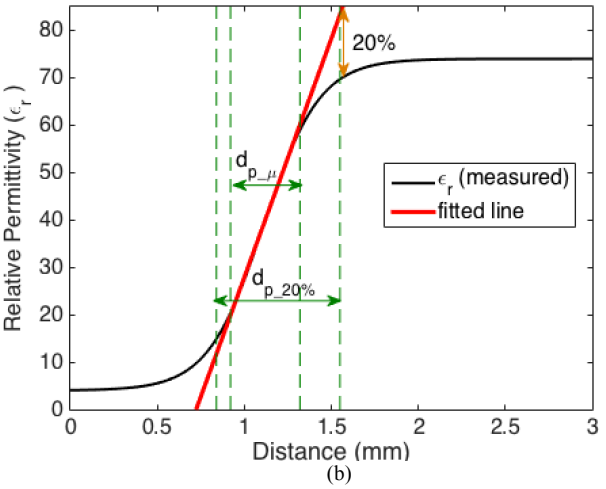

(b)

Fig. 5. Example data with candidate histology depth definitions marked. The plot is of measured relative permittivity (ε_r) vs. distance at a fixed frequency, with ε_{r1} and ε_{r2} denoting the relative permittivity of Materials 1 and 2, respectively, at this frequency. Note that d=0 mm is the measurement taken when the probe is in good contact with Material 1. (a) The sensing depth definitions from Section III.B. 1), 2), and 5) are marked on the figure as $d_{s\_10\%}$, d_{s_μ}, and d_{comb_μ}, respectively. (b) The penetration depth definitions from Section III.B. 3) and 4), are marked on the figure as $d_{p\_20\%}$ and d_{p_μ}, respectively; and the vertical, green lines indicate (from left to right) the distance at which the curve deviates from the fitted line by 20%, μ%, μ%, and 20%, respectively.

We note that for depths from d = 0 mm to where the region given by d_{comb_μ} starts, only Material 1 contributes to the permittivity measurement (the measured $\varepsilon_r = \varepsilon_{r1}$). If this distance and the distance d_{comb_μ} are to be included in the histological analysis, one may consider weighing the contribution of the various depths to account for this. However, this topic is not covered in this work and should be investigated in future studies. Further, while each of these depth concepts has been demonstrated using ε_r, they can equally be applied to conductivity measurements.

VI. Analysis and Results

In this section, we present the results of data collection and analysis. We start by showing some examples of measured data that are useful to understanding and interpreting the later analysis. Then, we examine the depths obtained from all five potential definitions for histology depth, for all tissue and phantom combinations based on a calculation involving the measured relative permittivity. Following this, we present the depths calculated based on the measured conductivity. Lastly, we compare the results and discuss the effect of various factors on the calculated depth values. In particular, we examine the three variables (depth definition, material properties and contrast, and measurement frequency) to determine if the calculated depth values depend on these variables.

A. Calculated Depth Results

First, we present an example that shows how the measured relative permittivity varies as the distance d increases. In Fig. 6, twenty measurements taken at 300 MHz with different distances between the probe tip and Material 1, for a porcine fat sample immersed in refined fat (Set #6). The plot demonstrates that the range of relative permittivity values over distance is equivalent to the range limited by the properties of the two materials. More specifically, when the probe is in contact with Material 1 (porcine fat sample), the measured relative permittivity is equal to the known relative permittivity (measured in isolation) of porcine fat (ε_{r1}), and when Material 1 is far from the probe (the probe is completely surrounded by Material 2) then the measured relative permittivity is equal to that of Material 2 (ε_{r2}). In between these distances, relative permittivity values fall within the range given by [ε_{r1}, ε_{r2}], and increase monotonically with increasing distance.

Next, we plot curves for the relative permittivity versus distance. As shown in Fig. 7, for a constant frequency, the measured relative permittivity over distance traces are approximately in the form of S-shaped curves. In this plot, individual measurements from Sets #2 and #6 are presented. The shape of these curves is representative of those of all Sets, although the initial and end relative permittivity values differ. There are two types of curves: one that starts at low

permittivity and increases with distance is obtained when Material 1 has lower relative permittivity than Material 2 (exemplified by Set #2 in Fig. 6); and one that starts at high relative permittivity and decreases with distance obtained when Material 1 has higher relative permittivity than Material 2 (as with Set #6).

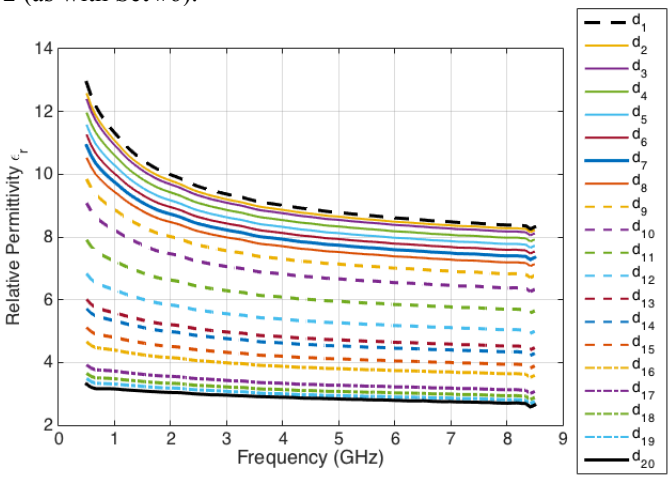

Fig. 6. An example measurement (Set #6) with refined fat as Material 1 and porcine fat as Material 2: plot of relative permittivity versus frequency for several separation distances of the probe and Material 1. The separation distances are labeled d_1:d_{20}, and the distance increases following the labeling. At distance d_1, the probe is in contact with the porcine fat. At distance d_{20}, the probe is surrounded entirely by refined fat. It is seen that by changing the separation distance, all relative permittivity values between those of the two materials may be measured.

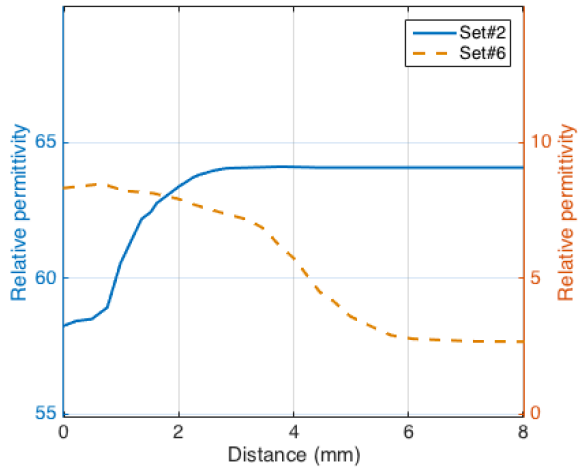

Fig. 7. Plot of a single measurement of relative permittivity versus distance at a frequency of 8.5 GHz for: Set #2 (solid blue line) demonstrating a lower permittivity material for Material 1 than for Material 2; and Set #6 (dashed orange line) demonstrating a higher permittivity Material 1 with a lower permittivity Material 2. Note that the y-axes differ. Depending on the relative material properties, the curve of relative permittivity versus distance can either trend to increasing or decreasing permittivity.

In Fig. 8, we present the full series of depths calculated based on the measured relative permittivities. For each of the six measurement Sets (as described in Table I), the five calculated depths are plotted for the lowest measurement frequency (300 MHz, in Fig. 8(a)), and for the highest measurement frequency (8.5 GHz, in Fig. 8(b)).

Next, we plot similar results from the point-of-view of the measured conductivity. Here, the conductivity is used to calculate the candidate histology depths in place of the relative permittivity, and for definitions involving the measurement uncertainty the uncertainty value for the conductivity measurement is now used. In Fig. 9, we present an example of a single measurement of conductivity versus distance from each of two Sets. This figure illustrates that the conductivity curves are very similar in shape and trend to the relative permittivity curves.

Finally, in Fig. 10 we present the result of the five candidate depth calculations based on the measured conductivity for each measurement Set. We expect that the depth calculations based on the measured conductivity are somewhat less reliable than the ones based on the measured relative permittivity, as the measurement uncertainty in the conductivity is higher.

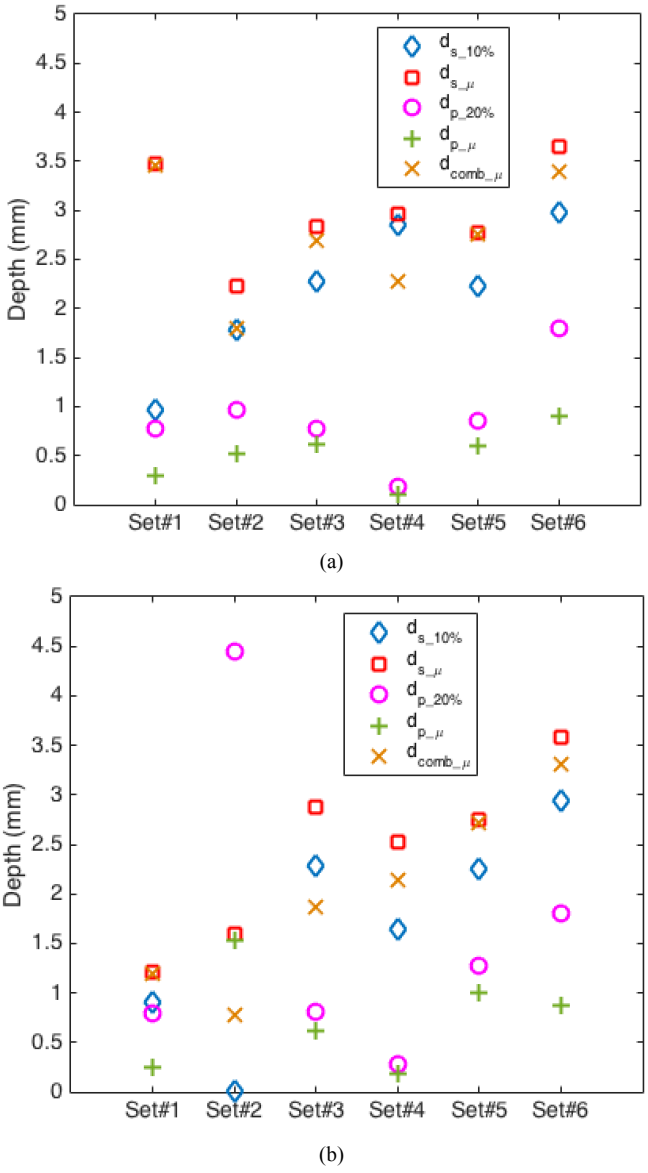

Fig. 8. Plot of the depth found from each of the five definitions, calculated using the measured relative permittivity, for all 6 Sets: (a) at 300 MHz, and (b) at 8.5 GHz. In these graphs, the blue diamond indicates $d_{s\_10\%}$, the red square d_{s_μ}, the pink circle $d_{p\_20\%}$, the green '+' d_{p_μ}, and the orange cross d_{comb_μ}, respectively. It is clear that different candidate histology depth definitions result in different calculated values.

B. *Dependence of Depth on Chosen Definition*

For calculations based on the relative permittivity, at 300 MHz (Fig. 8(a)), the smallest depth is 0.106 mm, given by d_{p_μ} for Set #4. The largest calculated depth found for this frequency is 3.646 mm for the d_{s_μ} of Set #6. In all cases, the definition d_{p_μ} leads to the smallest depth, followed by $d_{p\_20\%}$. The remaining three definitions ($d_{s\_10\%}$, d_{s_μ}, d_{comb_μ}) have more variable outcomes; however, they are always the three greatest depths. At 8.5 GHz, as in Fig. 8(b), the smallest depth is found to be only 0.001 mm, given by $d_{s\_10\%}$ (Set #2). In all Sets other than #2, d_{p_μ} gives the smallest depth followed by $d_{p\_20\%}$, as with 300 MHz. The largest recorded depth at this frequency is 4.45 mm, for $d_{p\_20\%}$ of Set #2.

For calculations based on the measured conductivity (as shown in Fig. 10), as with the depths based on the measured relative permittivity, the smallest depth across all frequencies is given by d_{p_μ}. Aside from Set #2 at 8.5 GHz, the second smallest depth for the remaining scenarios is given by $d_{p\_20\%}$. The largest depth is generally obtained from the d_{comb_μ} or d_{s_μ} calculations.

Finally, the difference in magnitude of the calculated depths, Δd, can be calculated for various scenarios. In this section, we examine a given Set (material combination) and frequency, and calculate the difference of the maximum depth over all definitions less the minimum depth over all definitions. For Sets #1-6 at 300 MHz, Δd is found to vary across the range [1.71, 3.17] mm as shown in Fig. 8(a)). As the histology depth used in the literature is generally on the order of several millimetres [14], [15], [17], the difference in these values for Δd are not insignificant. Thus, it is clear that the calculated depth varies appreciably based on the definition used. This data emphasizes that if different definitions are used, the resulting histology region and its corresponding tissue composition may vary widely. As such, a single definition is required to ensure consistency in results across studies.

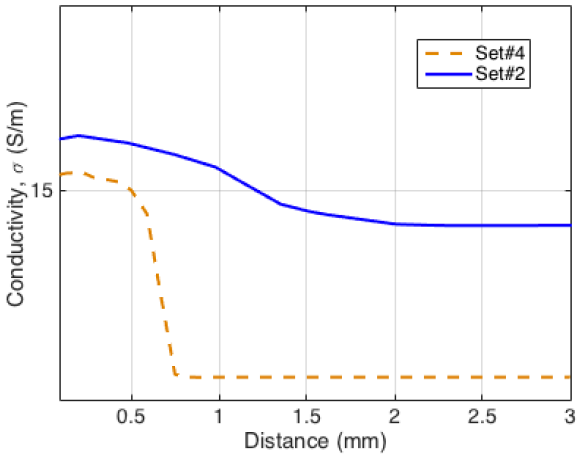

Fig. 9. Measured conductivity versus distance for single representative measurements at 8.5 GHz, from: Set #2 (solid blue line; low contrast in material properties) and Set #4 (dashed orange line, high contrast in material properties).

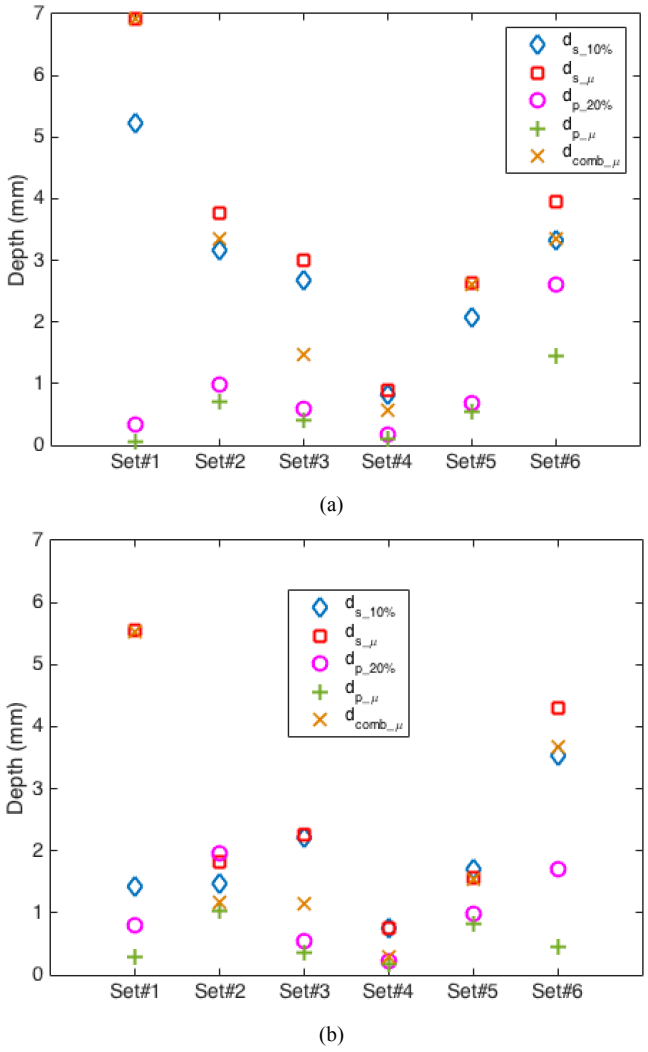

Fig. 10. Plot of the depth found from each of the five candidate histology depth calculations using the measured conductivity, for all 6 Sets: (a) at 300 MHz, and (b) at 8.5 GHz. In these graphs, the blue diamond indicates $d_{s\_10\%}$, the red square d_{s_μ}, the pink circle $d_{p\_20\%}$, the green '+' sign d_{p_μ}, and the orange cross d_{comb_μ}, respectively.

C. *Dependence of Depth on Material Properties*

Next we look at the effect of material properties on the calculated depth values. In particular, the properties encompass the complex permittivity of Material 1, the complex permittivity of Material 2, and the relative dielectric contrast between the materials. As the dielectric properties of tissues are dispersive with frequency, the individual material properties and the contrast may also vary with frequency. We discuss the relationship between depth and frequency in more detail in the next section. However, in this section, we first look at the effect of fixing both the depth definition and the frequency, to see how the depth compares across various material combinations.

With a fixed depth definition and a fixed frequency, for example, d_{s_μ} at 8.5 GHz as in Fig. 8(b), the calculated depth across all material combinations (i.e., across all measurement Sets), varies from 1.20 mm (Set #1) up to 3.59 mm (for Set #6). For $d_{p\_20\%}$ from the same plot, the depth value varies

across sets by more than 4.18 mm. Similarly, for $d_{s\_10\%}$, the calculated depth varies by 2.94 mm. As can be seen from Figs. 8 and 10, there are no depth definitions that result in consistent depth values regardless of the properties of the materials being measured.

We further investigate the effect of material properties by examining a specific case scenario. At 8.5 GHz, as in Fig. 8(b), the smallest depth $d_{s\_10\%}$ is found to be only 0.001 mm with the measurement of Set #2. This represents a special case, where the definition for $d_{s\_10\%}$ almost fails. In particular, for these materials at this frequency, the relative permittivity of Material 2 decreased by 10% (according to the definition for $d_{s\_10\%}$) is very nearly equal to the relative permittivity of Material 1 (there is a very low contrast of only 1.1:1 in their respective dielectric properties). At the lower frequency of 300 MHz, the contrast was higher and the depth $d_{s\_10\%}$ was calculated to be 1.77 mm. From these results, it is evident that the contrast between the two materials and their relative properties has an impact on all depth definitions.

The effect of material properties can also be seen in Figs. 7 and 9, in the plots of permittivity or conductivity versus frequency for various measurement Sets. Particularly in Fig. 9, the data shows that the change in measured properties may occur quickly (when a large contrast is present between the two materials) or very gradually (when a low contrast exists). With all depth definitions, generally a very gradual transition region will result in larger calculated depth values than a sharp transition.

From all of these results, it is evident that the contrast between the two materials and their relative properties has an effect on all of the candidate histology depth definitions.

D. Dependence of Depth on Frequency

As noted in the previous subsection, the dielectric properties of biological tissues are frequency-dependent. This suggests that depth calculations may also be frequency-dependent. Next, we investigate the change in calculated depth with frequency, for fixed depth definitions and fixed material Sets.

In Fig. 11, we plot the difference in calculated depths across frequency. More specifically, this change in depth is calculated as the absolute value of the difference between depth values at 8.5 GHz (Fig. 8(b)) and 300 MHz (Fig. 8(a)), for each measurement Set and each definition. From Fig. 11, it is seen that for some measurement Sets (i.e., some material combinations), the change in depth with respect to frequency is small – as in the case of Set #5 and Set #6. In particular, for every depth definition applied to the measurements of Set #6, the change with frequency is negligible. In other cases, the change in calculated depth with frequency is higher. The maximum difference in calculated depths is found with the penetration depth definition, $d_{p\_20\%}$, for the Set #2 measurement, in which the difference in calculated depth between 300 MHz and 8.5 GHz is 3.5 mm.

To explore what causes a calculated depth to be dependent on frequency, we delve further into the two extremes shown in Fig. 11: Set #2, which has the highest change in calculated depth with respect to frequency; and Set #6, which has the smallest change with respect to frequency. In Set #6, the materials being measured are raw porcine fat and refined fat. Both fat tissues have low permittivity and low loss. We hypothesize that the depth values resulting from the various definitions do not vary significantly with frequency for this material combination since the fat tissues have dielectric properties that are relatively constant with frequency over this range as compared to other tissues.

In Set #2, a high permittivity phantom is measured with a background of saline (also high permittivity). In this measurement scenario, there exists a cross-over in material properties with respect to frequency. In other words, at low frequencies, Material 1 has a higher permittivity than Material 2. However, at higher frequencies, Material 2 has the higher permittivity. At lower frequencies the contrast in material properties is also greater than at higher frequencies. As a result, the calculated depth for this measurement scenario depends on frequency regardless of the definition used. As Material 1 is a phantom material, the dielectric contrasts may not precisely represent those of actual tissue compositions. Despite this, the results of Set #2 demonstrate explicitly that the effect of frequency on the depth should be considered carefully. In particular, the extent of the dielectric properties dispersion with frequency, and the rate of change with frequency of the properties of Material 1 relative to those of Material 2 can affect the depth calculation for all definitions considered here.

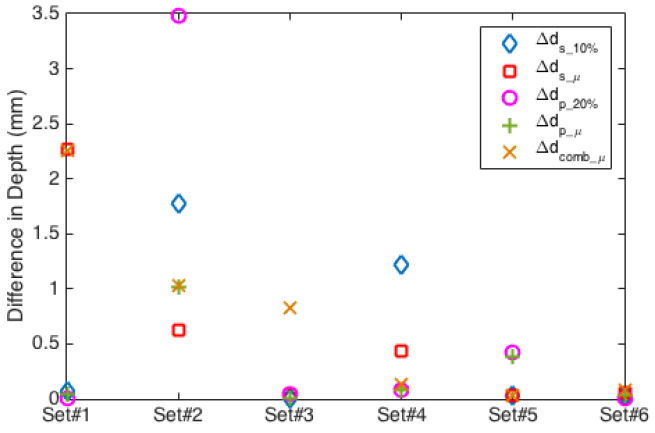

Fig. 11. The difference in depths across frequency (given by the absolute value of the difference between the depth calculated at 300 MHz and at 8.5 GHz for each definition). In this graph, the blue diamond indicates the difference in $d_{s\_10\%}$, the red square d_{s_μ}, the pink circle $d_{p\_20\%}$, the green '+' d_{p_μ}, and the orange cross d_{comb_μ}, respectively.

E. Discussion and Selection of Histology Depth Definition

Overall, we can conclude several points based on the results of this investigation. Primarily, the calculated depth value is highly dependent on the specific definition used. We have also found that the calculated value depends on the measurement scenario (i.e., the material properties and the dielectric contrast between them) for all depth definitions. Finally, while the depth may be relatively independent of frequency in certain situations, there are also situations in which it is frequency-

dependent as a result of the changing dielectric contrast with frequency.

In order to apply these findings to a dielectric measurement of a heterogeneous tissue, it is evident that careful consideration should be given to selecting the appropriate histology depth definition based on the experimental motivation. Without such consideration, especially with more complex tissue compositions, it may be difficult to assess the results in any meaningful way.

We recommend defining the histology depth as being equivalent to the d_{s_μ} sensing depth. This proposed sensing depth definition is by far the best option out of the ones considered. First, taking d_{s_μ} as the histology depth takes into consideration the uncertainty levels of the measurement. Further, d_{s_μ} is based entirely on measured parameters, without any arbitrary parameter selection (unlike the $d_{p\_20\%}$ and $d_{s\_10\%}$ definitions from the literature). Finally, d_{s_μ} also includes d = 0 mm (the probe contact point), ensuring that the tissue that contributes most significantly to the measurement is included in the histological analysis.

By defining the histology depth as being equal to d_{s_μ}, the region of tissue that is analysed histologically is the same region of tissue that contributes to the dielectric measurement data. This region is also the minimum sample thickness that is require to measure only the sample (i.e., not the container or holder behind it). In other words, if the histology depth was chosen to be a value $d_1 < d_{s\_\mu}$, then there is a region of tissue beyond d_1 which is not considered in the histological analysis but does contribute to the dielectric data. If the tissue sample was sliced horizontally at d_1 and dielectric data was taken with the sample backed by metal or air, the dielectric measurement would change as compared to the unsliced sample. On the other hand, if the histology depth is chosen to be $d_2 > d_{s\_\mu}$, then the histological analysis covers a region larger than that which contributes to the dielectric measurement. In either scenario, the types of tissues present within the histology region and their relative proportions do not accurately correspond to the tissues which resulted in the dielectric measurement. Therefore, d_{s_μ} provides the only histology depth that enables accurate correspondence between the dielectric data and the histological analysis.

Using the d_{s_μ} definition for the histology depth, we find that the histology depth varies from a minimum of 1.20 mm to a maximum of 3.65 mm, depending on the frequency and materials involved. We also note that the histology depth is expected to vary with sample temperature, as the temperature has an impact on the dielectric properties. Furthermore, this histology depth definition should be used with the caveat that the regions within the extent of the sensing depth may need to be weighted differently, with the tissue in closest proximity to the tip of the probe being the dominant contributor to the measured dielectric properties. It may be prudent to select the depth post-histological analysis, based on the tissue constituents and layout within the tissue sample. In this way, performing histological analysis on the first ~4 mm of tissue will enable extracting the histology of the desired histology region regardless of the measurement scenario. Further studies should be performed in order to investigate the optimal solution for identifying the histology depth based on the processed slices of a given sample, and to quantitatively determine how materials at different depths within the histology depth contribute to the measured properties.

VII. Conclusion

In this work, we have investigated the extent into a tissue sample that is considered for histological analysis in relation to dielectric measurements. This histology depth is a key parameter in interpreting dielectric measurements of heterogeneous tissues, as it must be clear which portions of the tissue sample and thus, what tissue types, have contributed to the dielectric property measurements. We have investigated potential ways to define the histology depth, and identified what we propose as the best possible definition. In the proposed definition, the histology depth is given by the depth to which the probe can detect changes in the tissue sample, within the measurement uncertainty. As a key result of this investigation, this proposed definition of histology depth can be used to consistently, and reliably, calculate the histology depth across experiments and studies.

The histology depth is found to vary with frequency, as expected as the tissue material properties themselves are frequency-dependent. In particular, the histology depth for a given tissue sample can change by as much as 2.27 mm over the frequency range of 300 MHz to 8.5 GHz. The histology depth also varies with the material properties and the dielectric contrast between them. The histology depth differs across all material types by up to 2.4 mm. These findings are significant, as they indicate that the histology depth may have been a confounder in historic data sets where the histology depth was taken as a constant value across all types of samples. Further, the findings in this study agree with recent literature in indicating that tissues at different distances from the probe tip do not contribute equally, or proportionally, to the measured dielectric properties. As a result, the tissue content may need to be weighted by distance from the probe.

However, this work has provided only the basis for histology depth studies. Additional measurements, conducted on a wide variety of biological tissue types, should be undertaken to confirm that these results apply across all tissues. Similarly, measurements should also be conducted on tissue samples that are highly heterogeneous (as opposed to layered stacks of homogeneous tissues) to further validate these findings. It is also important to note that the calculation of histology depth will likely vary based on the tissue temperatures (which affects their dielectric properties), the type and diameter of probe used. In future work, research will be undertaken in order to determine how to model, and numerically account for, the topmost tissue layer having the most dominant impact on the measured properties. At the same time, studies will be conducted to examine the histology radius under various realistic scenarios. Lastly, studies on how to associate histological findings of heterogeneous tissues with dielectric data (including weighing of tissues versus their

distance radially and longitudinally from the probe) will be performed to fully characterize this correspondence.

ACKNOWLEDGMENT

The authors thank P. M. Meaney of Dartmouth College for his support and discussions related to this research. We are grateful to A. Santorelli and M. Popovic of McGill University, Canada, for supplying the tissue-mimicking phantoms used in this study. We also thank I. Merunka of Czech Technical University, Prague, Czech Republic, for his input on the uncertainty analysis of the system.

REFERENCES

[1] S. Gabriel, R.W. Lau and C. Gabriel, "The dielectric properties of biological tissues: II. Measurements in the frequency range 10 Hz to 20 GHz," *Phys. Med. Biol.,* Vol. 41, pp. 2251-2269, 1996.

[2] K. R. Foster, J. L. Schepps, R. D. Stoy, and H. P Schwan, "Dielectric Properties of Brain Tissue Between 0.01 and 10 GHz," *Phys. Med. Biol*., vol. 24, no. 6, pp. 1177-1187, 1979.

[3] M. Lazebnik, M. C. Converse, J. H. Booske, and S. C. Hagness, "Ultrawideband temperature-dependent dielectric properties of animal liver tissue in the microwave frequency range," *Phys. Med. Biol*., vol. 51, pp. 1941-1955, 2006.

[4] C. L. Brace, "Temperature-dependent dielectric properties of liver tissue measured during thermal ablation: Toward an improved numerical model," *30th Ann. Intl. Conf. IEEE Eng. Med. Biol. Soc. (EMBS),* Vancouver, Canada, Aug. 20-24, 2008.

[5] T. Sherertz and C. J. Diederich, "Hyperthermia in Locally Recurrent Breast Cancer," in Radiation Therapy Techniques and Treatment Planning for Breast Cancer, Springer International Publishing, Switzerland, 2016, Ch. 9, pp. 145-158.

[6] P. T. Nguyen, "Focusing Microwave Hyperthermia in Realistic Environment for Breast Cancer Treatment," Ph.D. Thesis, University of Queensland, 2015.

[7] P. T. Nguyen, A. Abbosh, and S. Crozier, "Microwave Hyperthermia for Breast Cancer Treatment Using Electromagnetic and Thermal Focusing Tested on Realistic Breast Models and Antenna Arrays," IEEE Trans. Antennas Propag., vol. 63, no. 10, pp. 4426-4434, 2015.

[8] A. Andreano, and C. L. Brace, "A comparison of direct heating during radiofrequency and microwave ablation in ex vivo liver," *Cardiovasc Intervent Radiol.*, vol. 36, no. 2, pp. 505-511, 2013.

[9] L. Farina, et al., "Characterisation of tissue shrinkage during microwave thermal ablation," *Int. J. Hyperthermia*, vol. 30, no. 7, pp. 419-428, 2014.

[10] W. Zhou, et al., "Comparison of Ablation Zones among Different Tissues Using 2450-MHz Cooled-Shaft Microwave Antenna: Results in *Ex Vivo* Porcine Models," *PLoS ONE*, vol. 8, no. 8, pp. 1-7, 2013.

[11] X. Nie, et al., "Numerical study of the effect of blood vessel on the microwave ablation shape," *Biomed. Mater. Eng.*, vol. 26, pp. S265-S270, 2015.

[12] R. C. Conceição, J. J. Mohr, and M. O'Halloran, "Tumor Classification," in An Introduction to Microwave Imaging for Breast Cancer Detection, 1st ed. Switzerland: Springer, 2016, ch. 5.

[13] M. Lazebnik, M. McCartney, D. Popovic, C. B. Watkins, M. J. Lindstrom, J. Harter, S. Sewall, A. Magliocco, J. H. Booske, M. Okoniewski, and S. C. Hagness, "A large-scale study of the ultrawideband microwave dielectric properties of normal breast tissue obtained from reduction surgeries," *Phys. Med. Biol.*, vol. 52, pp. 2637-2656, 2007.

[14] M. Lazebnik, D. Popovic, L. McCartney, C. Watkins, M. Lindstrom, J. Harter, S. Sewall, T. Ogilvie, A. Magliocco, T. Breslin, W. Temple, D. Mew, J. Booske, M. Okoniewski, and S. Hagness, "A large-scale study of the ultrawideband microwave dielectric properties of normal, benign and malignant breast tissues obtained from cancer surgeries," *Phys. Med. Biol*., vol. 52, no. 20, pp. 6093-6115, 2007.

[15] A. M. Campbell and D. V. Land, "Dielectric properties of female human breast tissue measured *in vitro* at 3.2 GHz," *Phys. Med. Biol.,* vol. 37, no. 1, pp. 193-201, 1992.

[16] T. Sugitani, et al., "Complex permittivities of breast tumor tissues obtained from cancer surgeries," *Appl. Phys. Lett.*, vol. 104, no. 253702, pp. 1-5, 2014.

[17] R. J. Halter, et al., "The correlation of *in vivo* and *ex vivo* tissue dielectric properties to validate electromagnetic breast imaging: initial clinical experience," *Physiol. Meas.*, vol. 30, pp. S121-S136, 2009.

[18] A. Sihvola, *Electromagnetic mixing formulas and applications.* London: IEE Publishing, 1999.

[19] P. M. Meaney, A. P. Gregory, N. Epstein, and K. D. Paulsen, "Microwave open-ended coaxial dielectric probe: interpretation of the sensing volume re-visited," *BMC Med. Phys*., vol. 14, no. 3, pp. 1-11, June 2014.

[20] W. T. Joines, Y. Zhang, C. Li, and R. L. Jirtle, "The measured electrical properties of normal and malignant human tissues from 50 to 900 MHz," *Med. Phys.,* vol. 21, pp. 547-550, 1994.

[21] S. S. Chaudhary, R. K. Mishra, A. Swarup, and J. M. Thomas, "Dielectric properties of normal and malignant human breast tissues at radiowave and microwave frequencies," *Indian J. Biochem. Biophys.,* vol. 21 pp. 76–79, 1984.

[22] D. M. Hagl, D. Popovic, S. C. Hagness, J. H Bookse, and M. Okoniewski, "Sensing Volume of Open-Ended Coaxial Probes for Dielectric Characterization of Breast Tissue at Microwave Frequencies," *IEEE Trans. Microw. Theory Techn.*, vol. 51, no. 4, pp. 1194-1206, Apr. 2003.

[23] Keysight Technologies, "85070E Dielectric Probe Kit 200 MHz to 50 GHz Technical Overview," 2015.

[24] P. M. Meaney, A. P. Gregory, J. Seppala, and T. Lahtinen, "Open-Ended Coaxial Dielectric Probe Effective Penetrative Depth Determination," *IEEE Trans. Microw. Theory Techn.*, vol. 64, no. 3, pp. 915-923, March 2016.

[25] Nephron, Wikimedia Commons, "Very high magnification micrograph of an acinic cell carcinoma," October 2016, [Online] https://commons.wikimedia.org/w/index.php?curid=17150203

[26] L. Abdilla, C. Sammut, and L. Z. Mangion, "Dielectric properties of muscle and liver from 500 MHz – 40 GHz," *Electrom. Biol. Med.*, vol. 32, no. 2, pp. 244-252, 2013.

[27] V. Lopresto, R. Pinto, G. A. Lovisolo, and M. Cavagnaro, "Changes in the dielectric properties of *ex vivo* bovine liver during microwave thermal ablation at 2.45 GHz," *Phys. Med. Biol., vol.* 57, pp. 2309-2327, 2012.

[28] C. Gabriel, and A. Peyman, "Dielectric measurement: error analysis and assessment of uncertainty," *Phys. Med. Biol.*, vol. 51, pp. 6033-6046, 2006.

[29] NIST Technical Note 1297, "Guidelines for Evaluating and Expressing the Uncertainty of NIST Measurement Results," ed B. N. Taylor and C. E. Kuyatt (Washington, DC: United States Department of Commerce), 1994.

[30] J. Garrett and E. Fear, "Stable and Flexible Materials to Mimic the Di-electric Properties of Human Soft Tissues", *Antennas Wireless Propag. Lett.*, vol. 13, pp. 599-602, 2014.

[31] A. Santorelli, O. Laforest, E. Porter, and M. Popović, "Image Classification for a Time-Domain Microwave Radar System: Experiments with Stable Modular Breast Phantoms," in *Proc. 9ih Eur. Conf. Antennas Propag. (EUCAP)*, Lisbon, Portugal, Apr. 12-17, 2015.